

Cross-intensity functions and the estimate of spike-time jitter

Richard H. R. Hahnloser

Received: 4 September 2006 / Accepted: 7 February 2007 / Published online: 27 March 2007
© Springer-Verlag 2007

Abstract Correlation measures are important tools for the analysis of simultaneously recorded spike trains. A well-known measure with probabilistic interpretation is the cross-intensity function (CIF), which is an estimate of the conditional probability that a neuron spikes as a function of the time lag to spikes in another neuron. The non-commutative nature of the CIF is particularly useful when different neuron classes are studied that can be distinguished based on their anatomy or physiology. Here we explore the utility of the CIF for estimating spike-time jitter in synaptic interactions between neuron pairs of connected classes. When applied to spike train pairs from sleeping songbirds, we are able to distinguish fast synaptic interactions mediated primarily by AMPA receptors from slower interactions mediated by NMDA receptors. We also find that spike jitter increases with the time lag between spikes, reflecting the accumulation of noise in neural activity sequences, such as in synfire chains. In conclusion, we demonstrate some new utility of the CIF as a spike-train measure.

1 Introduction

The most commonly used spike correlation measures are commutative, i.e., they are essentially unchanged by the combined operation of neuron interchange and time reversal. Examples of commutative measures are the cross-correlation function or joint spike density (Tuckwell 1988) and the coherency function (Jarvis and Mitra 2001). The cross-correlation function has a

probabilistic interpretation: it can be thought of as the joint probability of observing spikes in neuron S at some time lag of spikes in neuron T (Palm et al. 1988).

Usually little importance is attributed to numerical values of correlations and coherencies, except that they must be significant by some standard. Possibly, because of this lack of numerical interest, it has been largely ignored that commutative correlation measures are not ideal for spike train pairs with very different average firing rates. For example, if hypothetical neuron T fires a spike every second and hypothetical neuron S synchronously fires spikes every 10 s, then their peak correlation and peak coherency both are only 0.1. However, given that all spikes in neuron S are perfectly synchronized with spikes in neuron T, we might prefer to work with correlation measures that reflect this fact by assigning the maximal correlation value of 1.0 in such a situation.

The non-commutative correlation measures analyzed in this study are useful when anatomical or other data are available based on which the two spike trains (and neurons) can be distinguished. For example, the cross-intensity function (CIF) (Brillinger 1992; Perkel et al. 1967) is an estimate of conditional spike probability (CSP), i.e., the probability of a spike in neuron T (target) conditional on a spike in neuron S (source) at some time lag, Fig. 1a. Conditional probabilities can be large even when average firing rates in neurons S and T are very different from each other. For the example in the last paragraph, the peak spike probability of target neuron T conditional on spikes in source neuron S is 1.0, thus accounting for the perfect synchrony in these neurons. Note that the cross intensity function is not a hazard rate in the language of stochastic processes and so is not to be confused with the conditional intensity function (Brown et al. 2001).

R. H. R. Hahnloser (✉)
Institute of Neuroinformatics UZH/ETHZ,
Winterthurerstrasse 190, 8057 Zürich, Switzerland
e-mail: rich@ini.phys.ethz.ch

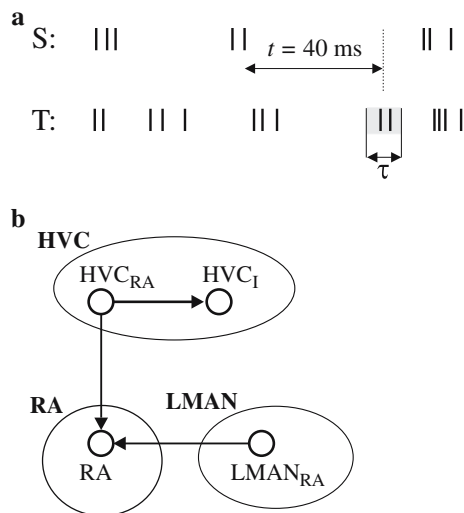


Fig. 1 **a** The (clipped) cross-intensity function (CIF, or CSP function) $P_{T|S}^{\tau}(t = 40 \text{ ms})$ is defined as the fraction of spikes in source neuron S that are followed by at least one spike in the target neuron T within the clipping window (gray area) of width τ . **b** The spike trains analyzed in this study are from two neuron classes in HVC (HVC_{RA} and HVC_I neurons), a neuron class in RA (RA neurons) and a neuron class in LMAN ($LMAN_{RA}$ neurons). Known synaptic connections are indicated by arrows. Known feedback connections from the inhibitory HVC_I neurons onto HVC_{RA} neurons are not plotted

To compensate for small amounts of data, it is common to reduce the temporal resolution of correlation functions, for example by temporal integration or by spike clipping (e.g., by clipping target spikes to time windows conditional on source spikes). Here we explore whether there exists a natural time scale over which one can integrate or clip CIFs. We find that when clipping is performed at the optimal width—defined by highest significance—we are left with a good estimate of temporal jitter between spike interactions. As a demonstration we apply CIF clipping to synaptically connected neuron classes and find that the optimal clipping width is small for neuron pairs interacting mainly through AMPA receptors, and large for neurons interacting through NMDA receptors—thus quite accurately reflecting receptor kinetics.

The data on which we illustrate the utility of CIFs are from simultaneous recordings of spontaneously active neurons in sleeping zebra finches (Hahnloser et al. 2006). We analyze spike trains from premotor neurons in HVC that project to the robust nucleus of the arcopallium (RA), and from RA neurons, Fig. 1b. RA neurons exhibit a regular background firing in the awake animal of about 20 Hz. During sleep, these neurons fire complex sequences of high-frequency bursts that can closely resemble premotor burst sequences recorded during singing (Dave and Margoliash 2000; Hahnloser

et al. 2002). The presence of bursting behavior throughout premotor song nuclei makes the sleeping bird an ideal system for the study of mechanisms of complex sequence generation and of synaptic interactions. The data are well suited for the exploration of CIFs thanks to the large variability of average firing rates (almost two orders of magnitude) and thanks to our knowledge of the underlying microcircuit that connects the different neuron classes (Fig. 2).

2 Results

Since our most interesting results were obtained with spike clipping, we restrict the presentation of our results to the clipped CIF. For results on the integrated CIF see the Methods section.

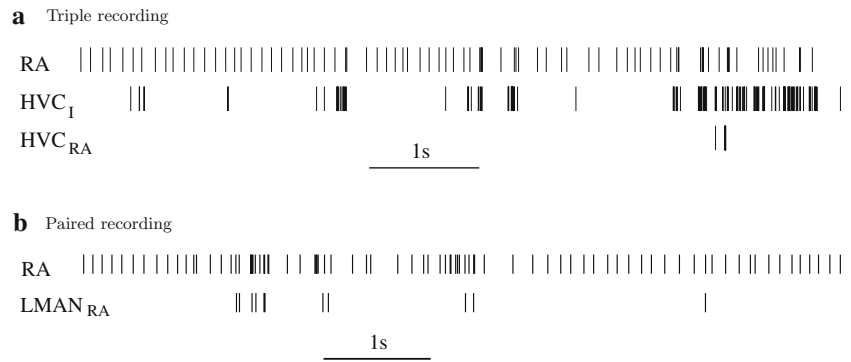
2.1 The clipped cross-intensity function

The (clipped) cross-intensity function $P_{T|S}^{\tau}(t)$ between spike trains produced by a ‘source neuron S’ and a ‘target neuron T’ is a function of time lag t . $P_{T|S}^{\tau}(t)$ assumes values between zero and one and is given by the fraction of spikes in the source neuron for which the target neuron fires at least one spike in the clipping window $[t - \tau/2, t + \tau/2]$ relative to source spikes. In other words, the variable t sets the offset of the clipping window from spikes in S and the parameter τ sets the width of the window, Fig. 1a.

Given a stationarity assumption, we can view the CIF at a particular time lag as an estimate of a binomial process, i.e., the probability of observing a target spike in a τ -window centered at time lag t of a source spike (see Methods). All time lags combined, the CIF forms estimates of many binomial processes, one for each time lag t . Because of this probabilistic interpretation, in the following we refer to the CIF also as the conditional spike probability (CSP) function.

When many target spikes are present within a clipping window, then these are reduced to a single event, thus guaranteeing that the CSP function is normalized between zero and one. If the clipping width τ is small, then conditional spike probabilities are very small, because few target spikes will be separated precisely by time lag t from a source spike. Small clipping windows may pose a problem because the estimation of small probabilities and their significance requires large amounts of data (see Methods). Therefore, it may be desirable to clip spike trains to much larger windows than the original sample time (which typically is 20–50 μs). However, very coarse clipping can be problematic as well. For example, for $\tau = 10 \text{ ms}$, if the target

Fig. 2 Example spike trains recorded in the sleeping zebra finch. **a** Triple recording of an RA, HVC_I, and HVC_{RA} neuron. **b** Paired recording of an RA, and an LMAN_{RA} neuron. Only small excerpts are shown here, spike trains analyzed were at least 200 s long



neuron forms a regular spike train of 100 Hz or higher, we have that every single clipping window will be filled with at least one target spike. Thus, we are left with the uninformative result $P_{T|S}^\tau(t) = 1$ irrespective of the source spike train. In conclusion, for given data the choice of the clipping window is subject to a tradeoff. Next we present a simple method for finding a suitable window size.

2.2 Confidence intervals and significance tests

A peak $\hat{p}^\tau = \max_t P_{T|S}^\tau(t)$ in the CSP function is indicative of interactions between two neurons, or their dependence on a common source signal (we keep the superscript τ as a free parameter). Peaks have to be tested for their significance as they can arise by chance even for mutually independent spike trains. A simple null hypothesis H_0 for significance tests is the assumption of independence of target spike probability and source spike times, $H_0 : \hat{p}^\tau = P_T^\tau$, where P_T^τ is the marginal spike probability, i.e., the probability that at least one target spike is observed in a random clipping window of width τ .

How can we determine whether to reject the null hypothesis or not? We choose as our test statistic the z -value function $z^\tau(t)$, defined as the difference between $P_{T|S}^\tau(t)$ and P_T^τ , normalized by the standard error of the CSP estimate (see Eq. 11 in the Methods section). When we assess the significance of a CSP peak \hat{p}^τ , we refer to this normalized difference simply as the z -value \hat{z}^τ . In general, the more source spikes we record, the more likely it is that a large deviation of \hat{p}^τ from P_T^τ will be significant.

2.3 An artificial example

In Fig. 3 we have created two artificial spike train pairs based on given CSP functions used as generative models. In both cases, the source neuron fires a spike exactly every second and the target neuron randomly fires a

spike in response to 70% of source spikes. The target spike times are randomly drawn from a Gaussian or a uniform probability density, centered on source spikes, Fig. 3a. We use these two spike train pairs to illustrate some of the properties of CSP functions.

The clipping width τ is an important parameter. Because both the marginal spike probability P_T^τ and the CSP $P_{T|S}^\tau(t)$ are monotonic functions of τ , their normalized difference—the z -value function $z^\tau(t)$ —may in fact be a non-monotonic function of τ . Indeed, the optimal clipping window $\hat{\tau} = \arg \max_\tau \hat{z}^\tau$ for the artificial spike trains is $\hat{\tau} \simeq 10$ ms, Fig. 3b (bottom). Because 10 ms also corresponds to the time jitter we artificially applied to the target spikes, we find that the optimal clipping window (defined as the window that yields highest significance) forms a good estimate of the temporal jitter of target spikes relative to source spikes. Note that a similar behavior of significance has been reported for a symmetric measure of spike coincidence as a function of coincidence width (Grün et al. 1999).

2.4 Application to songbird data

We applied our methods to real spike trains recorded in the sleeping songbird. We used previously published data from neuron pairs in premotor area HVC and the robust nucleus of the arcopallium (RA). In HVC, data were derived from sparsely firing excitatory neurons projecting to RA (HVC_{RA} neurons, abbreviated H) and from inhibitory HVC interneurons (HVC_I neurons, abbreviated I). We also used data records from a single RA neuron class of excitatory neurons (RA neurons, abbreviated R).

Our first analysis was to study CSP functions of HVC_{RA} and RA neuron pairs. Conditional on spikes in HVC_{RA} neurons, we usually observed several significant peaks in CSP functions, Fig. 4a. The peak CSP \hat{p}^τ increased steeply as a function of clipping width, reaching a plateau within less than 10 ms, Fig. 4b (top). For this CSP peak, we plotted the z -value \hat{z}^τ and found a distinct

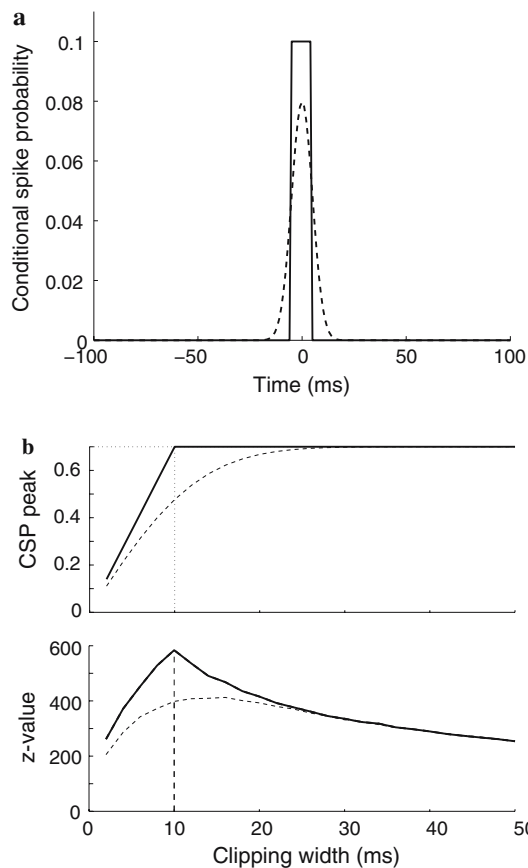


Fig. 3 Two artificial examples where given conditional spike probability functions are used to generate spike trains. **a** In the first example the probability density of a target spike as a function of the time lag to source spikes is a box function (*full line*); in the second example it is a Gaussian (*dashed line*). The width of the box function and the standard deviation of the Gaussian density both are 10 ms. The area under each curve is 0.7. **b** The peak CSP \hat{p}^τ is a monotonically increasing function of the clipping width τ (*top*). The peak z-value \hat{z}^τ (*bottom*) is a non-monotonic function of τ and peaks at roughly 10 ms for both the box function (*full line*) and the Gaussian (*dashed line*)

maximum for a clipping window of 4.0 ms, Fig. 4b (bottom). After examining a larger population of HVC_{RA}–RA neuron pairs, we found that optimal clipping windows had a median value of 4 ms (range 0.2–47.8 ms, $n = 46$ HVC_{RA}–RA neuron pairs). These results suggest that the drive provided by HVC_{RA} neurons onto RA neurons is subject to a small temporal jitter of only ± 2 ms.

Analyzing HVC_{RA}–HVC_I neuron pairs, we found many significant CSP peaks close to zero time lag. Even though CSP functions near the peak were quite broad (10–100 ms), z-values reached a maximum for small clipping windows (of median value $\hat{\tau} = 5.0$ ms, range 1.4–48.4 ms, $n = 26$ neuron pairs). Note that for a clipping window of $\tau = 5$ ms, we found a large average CSP peak of $\langle \hat{p}^\tau \rangle = 0.61$ in these neurons.

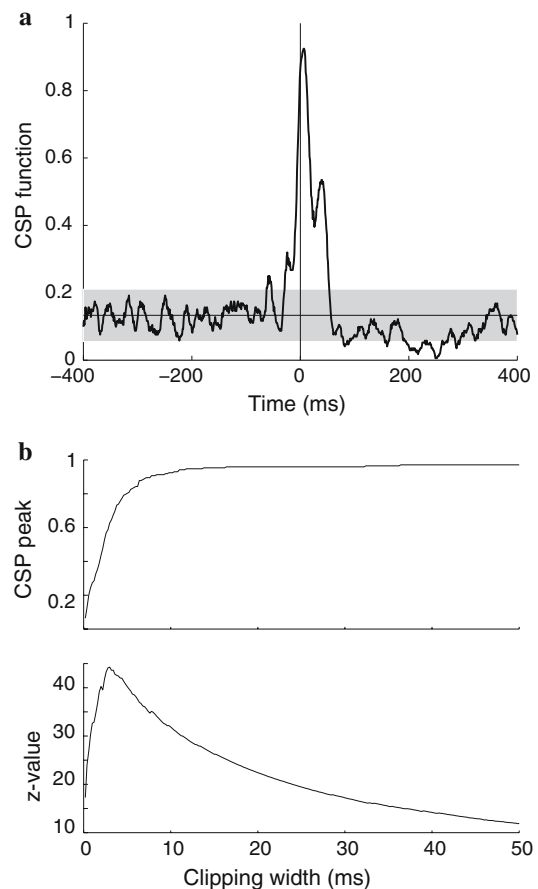


Fig. 4 HVC_{RA}–RA neuron pair. **a** CSP function $P_{RIH}^\tau(t)$ for $\tau = 5$ ms. The horizontal line indicates the marginal probability P_R^τ and the gray area delimits a confidence interval of 99% (a z-value of 2.33 corresponds to a significance level of $p = 0.01$). **b** *Top* the CSP peak \hat{p}^τ is a steep function of clipping width τ , saturating at a value close to one. *Bottom* the peak z-value \hat{z}^τ peaks at roughly 4 ms

The optimal clipping windows of HVC_{RA} neurons and their target neurons in HVC and RA are small, strongly suggestive of strong and precise synaptic interactions. In fact, values of $\tau = 4$ –5 ms are in agreement with time constants of fast AMPA receptor kinetics. AMPA is known to be the dominant receptor type of HVC_{RA} neuron synapses in adult birds (Mooney and Konishi 1991; Stark and Perkel 1999).

To further explore the relationship between optimal clipping windows and known synaptic kinetics, we analyzed a set of paired recordings in LMAN and RA. RA-projecting neurons in LMAN (LMAN_{RA} neurons) are known to drive RA neurons by action of NMDA-type glutamate receptors (Mooney and Konishi 1991; Stark and Perkel 1999). In conditional correlation functions of 11 LMAN_{RA}–RA neuron pairs, we found that optimal clipping windows had a median width of 27 ms (range 2–76 ms). Note that the large clipping windows

associated with LMAN projection neurons cannot be explained by spike propagation times. In fact, in our previous antidromic stimulation experiments we found that the variability of spike latencies is smaller in LMAN_{RA} neurons (0.81 ms) than in HVC_{RA} neurons (2.4 ms) (Hahnloser et al. 2006). Note also that optimal clipping windows were not obviously related to presynaptic spike-train statistics, despite large differences between HVC_{RA} and LMAN_{RA} statistics. For example, HVC_{RA} neurons exhibited frequent bursts, whereas LMAN_{RA} neurons did not, Fig. 5c. The average optimal window was unchanged in HVC_{RA}–RA pairs (4 ms) when we removed all burst spikes in HVC_{RA} neurons, leaving only single spikes for the computation of CSP functions. And, the optimal clipping windows of LMAN_{RA}–RA pairs were smaller than the typical interspike intervals of LMAN_{RA} neurons, implying that spike statistics of single neurons cannot explain the clipping behavior of LMAN_{RA}–RA pairs. In conclusion, we attribute the large differences in optimal clipping windows between HVC and LMAN projection neurons mainly to kinetics differences of synaptic receptors. The large clipping windows for LMAN_{RA} neurons agree well with the slow action of NMDA receptors, and the smaller windows for HVC_{RA} neurons agree with the faster action of AMPA receptors, see the inset of Fig. 5c.

Given the precise drive provided by HVC_{RA} neurons onto target neurons in HVC and RA, we expected similarly precise spike correlations between the target neurons themselves. Indeed, optimal spike detection windows between RA and HVC_I neurons had a median value of 7.7 ms (conditional on RA neuron spikes, $n = 50$ neuron pairs, Fig. 6). Thus, the average spike time jitter between RA and HVC_I neurons is slightly larger than that of synaptically connected pairs such as HVC_{RA}–HVC_I and HVC_{RA}–RA pairs. In fact, such a behavior was to be expected, given that correlations between HVC interneurons and RA neurons can only arise indirectly via their common source (HVC_{RA} neurons). Quantitatively, assuming that noise sources responsible for spike-time jitter are independent among target neurons, we would have expected a spike jitter of 6.4 ms for RA–HVC_I neuron pairs ($6.4 \text{ ms} = \sqrt{4^2 + 5^2} \text{ ms}$), only slightly smaller than the measured value of 7.7 ms.

So far we have ignored a possible relation between time lags t and optimal clipping widths. These two variables may be correlated based on our interpretation of the optimal clipping window as an estimate of temporal jitter inherent in synaptic interactions. By the finite coherence time of stochastic processes and the accumulation of noise in serial computations, we expect temporal jitter to increase with increasing time lag between

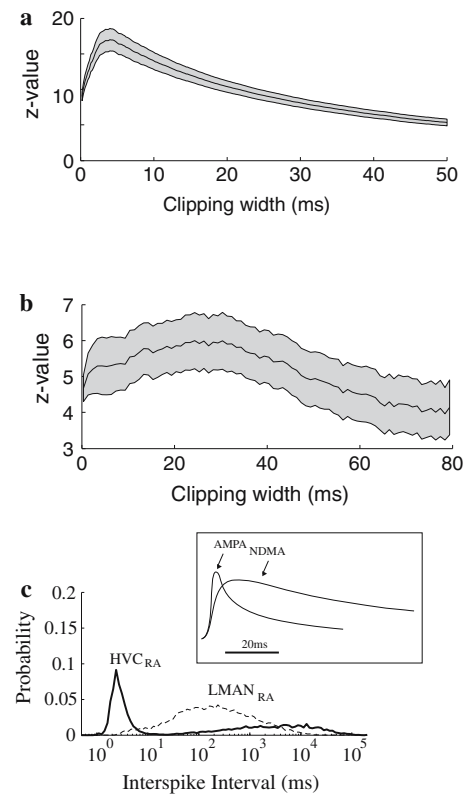


Fig. 5 The optimal clipping width reflects synaptic receptor time constants. **a** The peak z-value function averaged over 46 HVC_{RA}–RA neuron pairs peaks at $\tau = 4.0$ ms. The gray area delimits the standard error of the mean. **b** The peak z-value function averaged over 11 LMAN_{RA}–RA neuron pairs peaks at $\tau = 30$ ms. **c** Average interspike interval probability density functions of HVC_{RA} and LMAN_{RA} neurons showing pronounced bursts only in HVC_{RA} neurons. *Inset* Examples of evoked postsynaptic currents (EPSCs) in RA neurons triggered by electrical stimulation in HVC and in LMAN. During HVC stimulation, NMDA receptors were blocked in RA (AMPA curve) and during LMAN stimulation, AMPA receptors were blocked in RA (NMDA curve). The inset has been redrawn with permission from Stark and Perkel (1999)

spikes (in a random walk, the expected distance from the origin increases with the number of steps). In other words, we expect the optimal clipping window to be large when the CSP function peaks at a large time lag, and vice versa when the CSP function peaks at a small time lag.

In a first analysis, we computed the optimal clipping window as a function of time lag t , $\hat{\tau}(t) = \arg \max_{\tau} z^{\tau}(t)$. The mean optimal clipping function $\langle \hat{\tau}(t) \rangle$ for 50 RA–HVC_I neuron pairs reached a minimum at a time lag of $t = -4$ ms, Fig. 7a. Thus the temporal jitter of RA neuron spikes is minimal 4 ms after HVC_I neuron spikes. Interestingly, the mean curve is well approximated by the lines $\tau = \pm 2(t + 4 \text{ ms})$, which means that the optimal clipping window tends to grow twice as fast as the

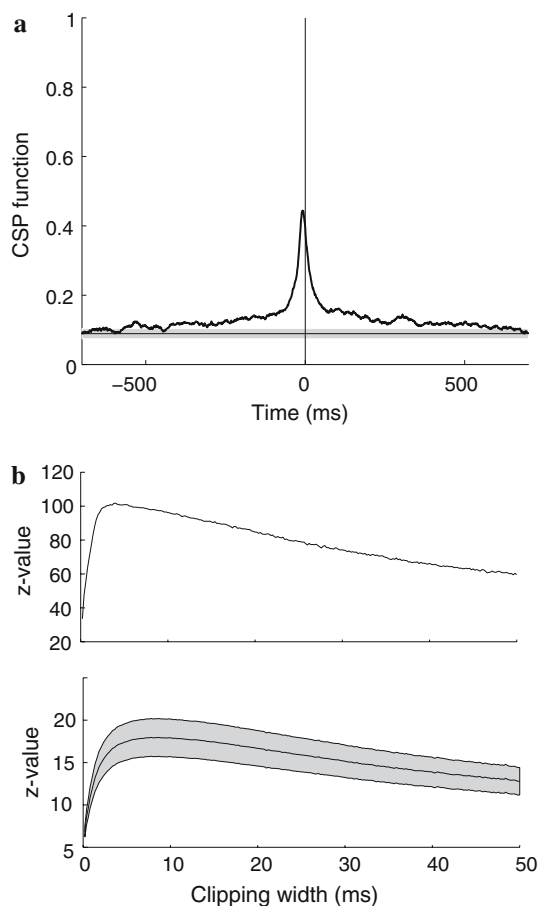


Fig. 6 RA–HVC₁ neuron pairs. **a** Example conditional correlation function $P_{IR}(t)$. Legend as in Fig. 4a. **b** Top the z-value function of this neuron pair. Bottom mean z-value function and standard error for $n = 50$ RA–HVC₁ neuron pairs

time lag. This behavior is suggestive of strong spike correlations at an exclusive time lag of -4 ms. Indeed, to include strongly correlated spikes at a lag of -4 ms, a clipping window centered at time lag t must have a halfwidth of at least $|t + 4|$ ms, which is what we observe.

By analyzing each neuron pair separately, we found that pairs with large optimal clipping windows have CSP peaks at large time lags. In a scatter plot of the optimal clipping window $\hat{\tau}$ versus the time lag $\hat{t} = \arg \max_t \hat{\tau}(t)$ at which optimality holds, we found a positive correlation with correlation coefficient $r = 0.52$ ($p < 10^{-4}$), Fig. 7b. Again, there is a tendency for the optimal window to grow twice as fast as the time lag of the CSP peak, indicating existence of a small and unique time lag at which strong spike correlations between RA and HVC₁ neurons exist.

To summarize these findings, we should slightly revise our original interpretation of the optimal clipping window as a simple estimate of spike-time jitter. That is, we must distinguish between true synaptic jitter of mono-

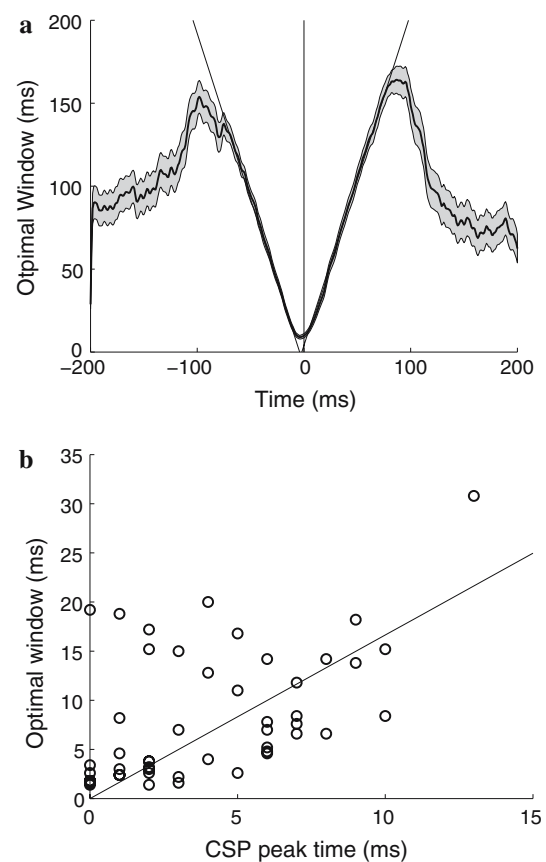


Fig. 7 **a** Optimal clipping width as a function of time lag. Shown is the optimal width $\hat{\tau}(t)$ averaged over $n = 50$ RA–HVC₁ neuron pairs. The standard error of the mean is shown in gray. The tilted black lines represent the curves $\hat{\tau}(t) = \pm 2(t + 4)$ ms. **b** Scatter plot of the optimal clipping width $\hat{\tau}$ versus $|\hat{t} - 4|$ ms for $n = 50$ RA–HVC₁ neuron pairs. The black line shows a linear regression curve

synaptic events (at small time lags), and the accumulation of jitter due to poly-synaptic events. Therefore, we should view the optimal clipping window at large time lags as an upper bound to the true (monosynaptic) jitter. We can estimate the true jitter by restriction of conditional spike probabilities to small time lags of a few milliseconds (if no spikes are present at small time lags, then precise estimation clearly is difficult).

2.5 Discussion

We have shown some new interesting properties of the cross-intensity function when spikes are clipped. Besides of providing for some smoothing, spike clipping can be used to estimate spike-time jitter from paired recordings of directly or indirectly connected neuron classes. We have found a correspondence between the optimal clipping window and the time constant of synaptic interactions. For NMDA-mediated synaptic interactions

optimal clipping windows are large, and for AMPA-mediated interactions they are small, in agreement with previous findings (Gutkin et al. 2003; Harsch and Robinson 2000). A similar use of the clipping operation has previously been demonstrated in a different context. By clipping artificial spike trains to variable bin sizes, Grün et al. were able to extract the applied temporal jitter to these spike trains using a commutative correlation measure (Grün et al. 1999, 2002). In agreement with a spike jitter estimate, we have found that optimal clipping windows typically are smaller than interspike intervals, and are also smaller than the widths of CSP peaks (which are a measure of co-fluctuation of firing rates—Figs. 4 and 6).

Our study leaves many open problems that need to be addressed in future work. For example, it can be argued that our significance test is based on too simplifying Poissonian assumptions. That is, we have estimated the marginal spike probability by the fraction of clipping windows that were filled with at least one spike. One can argue that a more stringent estimate might be more adequate. For example, given the strong tendency of HVC projection neurons to produce spike bursts, we might want to estimate the standard error S_T^r in Eq. 10 by the number of source bursts instead of the number of source spikes. As there always are fewer bursts than spikes, we would obtain an increased standard error and so be less likely to reject the null hypothesis of independence.

Even with this more stringent significance test, we may be strongly biased towards rejecting the null hypothesis. In an earlier study, we found that during sleep, firing rates of neurons are highly fluctuating on the time scale of seconds (Hahnloser et al. 2006). In this context, it is not clear whether significant peaks in CSP functions arise from true spike correlations, or from coincident fluctuations of excitability. To be able to distinguish fast spike-time correlations from slow correlations due to a common source of excitability, it might be possible to apply similar techniques as in (Brody 1999; Grün et al. 2002). The essential idea would be to use a local estimate of background correlation, thus reducing the sensitivity to nonstationarities in excitability. There exist powerful techniques to segment nonstationary spike trains into non-overlapping time windows during which spike train statistics are approximatively stationary (Danóczy and Hahnloser 2006; Grün et al. 2002). By first running such a segmentation analysis, we could restrict the entire analysis to segments with stationary spike train statistics only, thus getting rid of excitability fluctuations.

An important limitation of our work is that we have only presented methods for single trial data, well applicable to studies of spontaneous activity during sleep and in-vitro experiments. However, often, correlation

measures are used in the context of multiple experimental trials (Brown et al. 2004; Schreiber et al. 2004). A multiple trial situation arises when some sensory or other nerve stimulation is repeatedly applied. We believe that cross-intensity functions can be very useful also for multiple trial data. The generalization might pose some challenges such as the formulation of significance tests with marginal spiking probabilities that are time-dependent (stimulus-locked) functions.

In conclusion, there remain interesting open problems to be studied; their solutions will help to strengthen the ties between raw spike data, probabilistic models of synaptic interactions, and Bayesian computation in neural circuits.

3 Methods

We first introduce spike-train correlation measures at the temporal resolution of the sample rate. We then discuss two methods for reducing temporal resolution: one is to clip spikes, the other is to (linearly) integrate.

3.1 Spike-train correlations

Spike train: We represent a spike train $\rho(t)$ by a sum of delta functions,

$$\rho(t) := \sum_{i=1}^N \delta(t - t_i), \tag{1}$$

where N is the total number of spikes generated up to time T . We assume that time is sampled in discrete steps Δt smaller than the refractory period of action potentials. The discrete delta function is defined as $\delta(k\Delta t) = 0$ for all integers $k \neq 0$ and $\delta(0) = 1/\Delta t$.

Cross-correlation function: Assume we are given spike trains from two neurons T and S, with spike times t_i^T ($i = 1, \dots, N_T$), and t_i^S ($i = 1, \dots, N_S$). The cross correlation function $P_{TS}(t)$ between the two spike trains is defined as

$$P_{TS}(t) := \langle \rho_T, \rho_S \rangle(t) = \frac{1}{T} \int_0^T ds \rho_T(t+s) \rho_S(s). \tag{2}$$

Note that neuron T is not to be confounded with the total recording time T . In general, we are interested in the cross-correlation function in some small time interval $|t| \leq t_{\max} \ll T$. The reason for this limited range is that in most neural systems we do not expect correlations between spike trains to last for longer than about $t_{\max} \sim 1$ s. In this limit, the cross-correlation function is *commutative*, which means that there exists a combined symmetry of neuron exchange and time reversal,

$P_{TS}(t) = P_{ST}(-t)$. Thanks to this commutative property, the cross-correlation function can be thought of as the *joint probability density* of observing a spike in neuron S separated by time t from a spike in neuron T.

Cross-intensity function: In probability theory, the conditional probability between two random variables is defined as the joint probability divided by the marginal probability. Accordingly, the cross intensity function (CIF) is defined as:

$$P_{T|S}(t) := \langle \rho_T | \rho_S \rangle(t) = \frac{1}{\langle \rho_S \rangle} \langle \rho_T, \rho_S \rangle(t), \tag{3}$$

where $\langle \rho_S \rangle := N_S/T$ is the average firing rate of neuron S. A straightforward calculation shows that the CIF is an estimate of the conditional spike probability (CSP) that neuron T spikes at a time lag t of a spike in neuron S:

$$\begin{aligned} P_{T|S}(t) &= \langle \rho_T | \rho_S \rangle(t) \\ &= \frac{N_S}{N_S T \langle \rho_S \rangle} \int_0^T ds \sum_{i=1}^{N_S} \delta(s - t_i^S) \rho_T(s + t) \\ &= \frac{\Delta t}{N_S} \sum_{i=1}^{N_S} \rho_T(t_i^S + t) \\ &= \frac{\# \text{ S spikes separated by } t \text{ of a T spike}}{N_S}. \end{aligned}$$

Given this probabilistic interpretation of the cross-intensity function, it makes sense to call neuron S the source neuron and neuron T the target neuron.

Confidence intervals: To put error bars on the CIF, in line with our probabilistic interpretation, we assume that spikes in the target neuron are generated by a Bernoulli process. That is, we assume that at time lag t of a spike in the source neuron, spikes in the target neuron are generated with probability $P_{T|S}(t)$. Given the N_S trials, the standard error $S_{T|S}(t)$ of our probability estimate is

$$S_{T|S}(t) := \sqrt{\frac{P_{T|S}(t)(1 - P_{T|S}(t))}{N_S}}. \tag{4}$$

That is, $S_{T|S}(t)$ represents the uncertainty of the conditional spike probability function at timelag t .

Significance: To test for significance of the peak $\hat{p} = \max_t P_{T|S}(t)$, we use as null hypothesis that the target spike train is conditionally independent of the source spike train, $H_0 : \hat{p} = P_T$, where P_T is the probability that the target neuron spikes in a randomly selected bin,

$$P_T := \frac{N_T}{T/\Delta t} = \frac{N_T \Delta t}{T}. \tag{5}$$

Here $T/\Delta t$ corresponds to the total number of time bins covered in time T (typically a very large number).

Given a confidence level α , we reject the null hypothesis if \hat{p} —being an estimator of P_T —falls into the α -tail of the estimator density. Using the Gaussian approximation of the Bernoulli distribution, we reject the null hypothesis if

$$z\text{-value} := \frac{|\hat{p} - P_T|}{\sqrt{\frac{P_T(1-P_T)}{N_S}}} > z_\alpha, \tag{6}$$

where z_α is the z -value of the Gaussian distribution (for example $z_\alpha = 2.33$ corresponds to a one-sided test at confidence level $\alpha = 1\%$).

With Δt being equal to the sample time, most bins will end up being devoid of spikes, leading to very small (conditional) spike probabilities. In general, the estimation of small probabilities is undesirable, because it requires a relatively large number of source spikes, i.e., long recordings. As a rule of thumb, to estimate the probability p of a binomial process we should perform at least $N_S = \frac{9}{p(1-p)}$ coin flips, which is a function that diverges as $p^{-1/2}$ when $p \rightarrow 0$ (with this choice of N_S , we expect to see each side of the coin at least 9 times).

There are two reasons why we are interested in performing our analysis with larger bin sizes: One is to obtain better statistics, and the other is to explore whether there exists a natural time scale for conditional spike probabilities. In the following we present two alternative methods for increasing bin size, one is by clipping, the other by integration.

3.2 Clipped cross-intensity function

The clipped CIF $P_{T|S}^\tau(t)$ is an estimate of spike probability in time bins τ larger than the sample time Δt ; it is given by the fraction of spikes in the source neuron S, for which the target neuron T fires at least one spike in the window $[t - \tau/2, t + \tau/2]$ relative to source spikes.

$$P_{T|S}^\tau(t) := \frac{1}{N_S} \sum_{i=1}^{N_S} \Theta \left(\frac{\tau}{2} - \min_j |t_i^S + t - t_j^T| \right), \tag{7}$$

where $|\cdot|$ denotes the absolute value, and Θ is the Heaviside function (i.e., $\Theta(x) = 1$ if $x \geq 0$ and $\Theta(x) = 0$ otherwise). The parameter τ is referred to as the clipping width. If we choose $\tau = \Delta t$ in Eq. 7, then we get back the original definition of the CIF (Eq. 3), as there can be at most one spike in a window of size Δt . The clipped CIF is a monotonically increasing function of τ , as in large windows it is more likely to encounter at least one spike than in small windows. Note that large windows may contain many spikes; therefore, we clip spike trains as a simple means to maintain a probabilistic interpretation.

Confidence intervals: We compute confidence intervals for $P_{T|S}^\tau(t)$ using the Gaussian approximation of the binomial distribution (large N_S -limit). Accordingly, confidence intervals correspond to multiples of the standard error $S_{T|S}^\tau(t)$ of a Bernoulli process with parameter $P_{T|S}^\tau(t)$. In analogy to Eq. 4 we have that

$$S_{T|S}^\tau(t) := \sqrt{\frac{P_{T|S}^\tau(t)(1 - P_{T|S}^\tau(t))}{N_S}}. \tag{8}$$

For example, the interval $\pm 2.58 S_{T|S}^\tau(t)$ corresponds to a 99% confidence interval for the estimate of $P_{T|S}^\tau(t)$.

Marginal probability: Under clipping, the marginal spike probability P_T^τ corresponds to the probability that a random time window of width τ contains at least one target spike. We estimate P_T^τ by the fraction of filled windows within the recording of duration T ,

$$P_T^\tau := \frac{\tau}{T} \sum_{k=1}^{T/\tau} \Theta\left(\frac{\tau}{2} - \min_j |k\tau - t_j^T|\right), \tag{9}$$

where T/τ corresponds to the number of clipping windows. For τ not too large, the confidence interval for P_T^τ is much smaller than that of $P_{T|S}^\tau(t)$, because there are more windows of size τ in Eq. 9 than there are source spikes in Eq. 7. This explains why for significance testing we neglect uncertainties in our estimate of P_T^τ .

Significance test: When we estimate the marginal probability P_T^τ from only N_S trials (for significance testing) then the estimate is subject to a standard error

$$S_T^\tau := \sqrt{\frac{P_T^\tau(1 - P_T^\tau)}{N_S}}. \tag{10}$$

The conditional spike probability $P_{T|S}^\tau(t)$ is significantly larger than the marginal spike probability P_T^τ if it satisfies

$$z\text{-value function} = z^\tau(t) = \frac{|P_{T|S}^\tau(t) - P_T^\tau|}{S_T^\tau} > z_\alpha. \tag{11}$$

This significance criterion has an interesting dependence on τ . Since all of $P_{T|S}^\tau(t)$, P_T^τ , and S_T^τ are increasing functions of τ , the z -value function may be a non-monotonic function of τ , as we have seen in Figs. 3, 4, 5 and 6.

Removal of single spikes: Note that to compute CIFs for RA – HVC_I neuron pairs and to test for significance in Fig. 6b, we removed single spikes in all RA neurons (all spikes separated by more than 10 ms from both preceding and succeeding spikes). This procedure was motivated by reversible lesion studies, where it was found that only RA bursts are driven from HVC, not RA single spikes (Hahnloser et al. 2006). In support of this procedure, when we did not remove single spikes

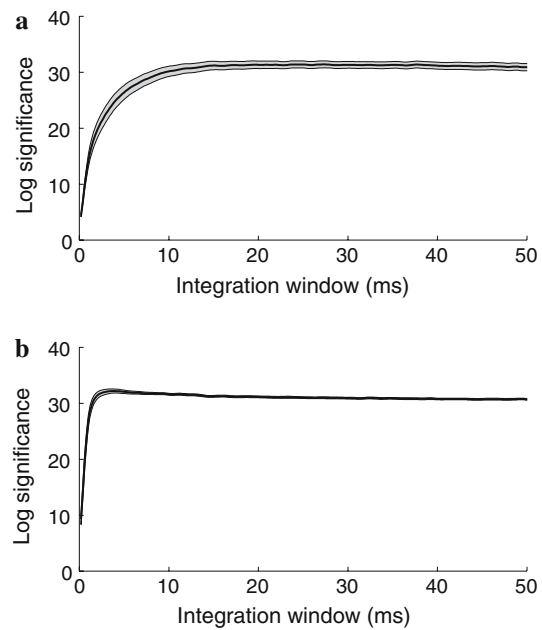


Fig. 8 Dependence of peak significance on the integration window size τ . For each τ and each neuron pair we have computed the integrated CIF $p^\tau(t) = P_{T|S}^\tau(t - \tau/2, t + \tau/2)$ as a function of t . Then we determined the peak $\hat{p}^\tau = \max_t p^\tau(t)$ and its log significance $s^\tau = -\log P(N > N_S \hat{p}^\tau | \hat{N})$. **a** Mean log significance (s^τ) for $n = 46$ HVC_{RA}–RA neurons as a function of the integration window size τ . **b** Mean log significance for $n = 50$ RA–HVC_I neurons. The gray areas delimit the standard error. Compare **a** and **b** with Figs. 5a and 6b where we used spike clipping instead of integration

in RA neurons, we did not observe significant correlations between CSP-peak time lags and optimal clipping windows in Fig. 7b.

3.3 Integrating the CIF

Instead of spike clipping, we can also integrate the (sample-time) CIF in Eq. 3 to obtain a lower-resolution estimate of conditional spiking. However, for the estimation of spike jitter the integrated CIF gave less satisfactory results than the clipped CIF, illustrated in the following.

Integrated CIF: To estimate the expected number of spikes $P_{T|S}(t_1, t_2)$ in neuron T in the time interval $[t_1, t_2]$ relative to a spike in neuron S, we have to integrate the CIF in Eq. 3 from t_1 to t_2 :

$$P_{T|S}(t_1, t_2) = \int_{t_1}^{t_2} P_{T|S}(t) dt.$$

We are interested in testing whether $P_{T|S}(t_1, t_2)$ is compatible with a null hypothesis H_0 of conditional independence of T spikes on S spikes: $H_0: P_{T|S}(t_1, t_2) =$

$(t_2 - t_1)P_T$, where the marginal probability P_T is defined as in Eq. 5.

According to this null hypothesis, the number of spikes in neuron T in $[t_1, t_2]$ is given by a cumulative Bernoulli process. If the probability per sample time of this process is very small and the interval $[t_1, t_2]$ extends over many sample times, then we may approximate the Bernoulli process by a Poisson process. We reject the null hypothesis at the α level if the probability of observing N_o spikes or more satisfies $P(N \geq N_o | \hat{N}) < \alpha$, where $N_o = N_S P_{T|S}(t_1, t_2)$ is the total number of T spikes in intervals $[t_1, t_2]$ and $\hat{N} = N_S(t_2 - t_1)P_T = N_S \frac{t_2 - t_1}{T}$ is the expected number of T spikes under hypothesis H_0 . To evaluate the probability $P(N > N_o | \hat{N})$ we make use of the incomplete gamma function as in (Grün et al. 2002).

We see in Fig. 8 that integrated CIFs lead to a qualitatively different behavior of significance than clipped CIFs. For HVC_{RA}–RA neurons the integrated CIF does not peak for small integration windows, but is an increasing function that reaches a plateau at roughly 15 ms, Fig. 8a. For RA–HVC_I neuron pairs a weak significance peak emerges at integration windows of roughly $t_2 - t_1 = 4$ ms, Fig. 8b. In general, we observed that integrated CIFs do not lead to sharp significance peaks, implying that integration is less suitable than clipping for inferring intrinsic time scales of neural interactions.

Acknowledgments We would like to thank Emery Brown for helpful discussions on cross-intensity functions.

This work was made possible by a professorship grant from the Swiss National Science Foundation.

References

- Brillinger DR (1992) Nerve cell spike train data analysis: a progression of technique. *J Am Stat Assoc* 87(418):260–271
- Brody CD (1999) Correlations without synchrony. *Neural Comput* 11:1537–1551
- Brown EN, Kass RE, Mitra PP (2004) Multiple neural spike train data analysis: state-of-the-art and future challenges. *Nat Neurosci* 7(5):456–461
- Brown EN, Barbieri R, Ventura V, Kaas RE, Frank LM (2001) The time-rescaling theorem and its application to neural spike train data analysis. *Neural Comput* 15:965–991
- Danóczy M, Hahnloser RHR (2006) Efficient estimation of hidden state dynamics from spike trains. In: Proceedings of NIPS2005—Neural information processing systems: natural and synthetic, Vancouver
- Dave AD, Margoliash D (2000) Song replay during sleep and computational rules for sensorimotor vocal learning. *Science* 290(5492):812–816
- Grün S, Diesmann M, Aertsen A (2002) Unitary events in multiple single-neuron spiking activity: I. Detection and significance. *Neural Comput* 14(1):43–80
- Grün S, Diesmann M, Aertsen A (2002) Unitary events in multiple single-neuron spiking activity: II. Nonstationary data. *Neural Comput* 14(1):81–119
- Grün S, Diesmann M, Grammont F, Riehle A, Aertsen A (1999) Detecting unitary events without discretization of time. *J Neurosci Methods* 94(1):67–79
- Gutkin B, Ermentrout GB, Rudolph M (2003) Spike generating dynamics and the conditions for spike-time precision in cortical neurons. *J Comput Neurosci* 15(1):91–103
- Hahnloser RHR, Kozhevnikov AA, Fee MS (2002) An ultra-sparse code underlies the generation of neural sequences in a songbird. *Nature* 419:65–70
- Hahnloser RHR, Kozhevnikov AA, Fee MS (2006) Sleep-related neural activity in a premotor and a basal-ganglia pathway of the songbird. *J Neurophysiol*. doi:10.1152/jn.01064.2005
- Harsch A, Robinson HP (2000) Postsynaptic variability of firing in rat cortical neurons: the roles of input synchronization and synaptic NMDA receptor conductance. *J Neurosci* 20(16):6181–6192
- Jarvis MR, Mitra PP (2001) Sampling properties of the spectrum and coherency of sequences of action potentials. *Neural Comput* 13(4):717–749
- Mooney R, Konishi M (1991) Two distinct inputs to an avian song nucleus activate different glutamate receptor subtypes on individual neurons. *Proc Natl Acad Sci USA* 88(10):4075–4079
- Palm G, Aertsen AM, Gerstein GL (1988) On the significance of correlations among neuronal spike trains. *Biol Cybern* 59(1):1–11
- Perkel DH, Gerstein GL, Moore GP (1967) Neuronal spike trains and stochastic point processes. II. Simultaneous spike trains. *Biophys J* 7(4):419–440
- Schreiber S, Fellous J-M, Tiesinga P, Sejnowski TJ (2004) Influence of ionic conductances on spike timing reliability of cortical neurons for suprathreshold rhythmic inputs. *J Neurophysiol* 91(1):194–205
- Stark LL, Perkel DJ (1999) Two-stage, input-specific synaptic maturation in a nucleus essential for vocal production in the zebra finch. *J Neurosci* 19(20):9107–9116
- Tuckwell HC (1988) Introduction to theoretical neurobiology, vol 2, chap 10, Cambridge studies in mathematical biology. University of Cambridge, Cambridge pp 243–246